Research in Astron. Astrophys. **2009** Vol. **9** No. **2**, 227–236
http://www.raa-journal.org *http://www.iop.org/journals/raa*

***R**esearch in*
***A**stronomy and*
***A**strophysics*

An optimal method for the power spectrum measurement *

Yi-Bin Yang[1,2], Long-Long Feng[2], Jun Pan[2] and Xiao-Hu Yang[3]

[1] Center for Astrophysics, University of Science and Technology of China, Hefei 230026, China; *fengll@pmo.ac.cn*
[2] Purple Mountain Observatory, Chinese Academy of Sciences, Nanjing 210008, China
[3] Shanghai Astronomical Observatory, the Partner Group of MPA, Nandan Road 80, Shanghai 20030, China

Received 2008 April 13; accepted 2008 May 20

Abstract An aliasing effect brought up by mass assignment onto Fast Fourier Transformation (FFT) grids may bias measurement of the power spectrum of large scale structures. In this paper, based on the Beylkin's unequally spaced FFT technique, we propose a new precise method to extract the true power spectrum of a large discrete data set. We compare the traditional mass assignment schemes with the new method using the Daub6 and the 3rd-order B-spline scaling functions. Our measurement of Poisson samples and samples of N-body simulations shows that the B-spline scaling function is an optimal choice for mass assignment in the sense that (1) it has a compact support in real space and thus yields an efficient algorithm (2) without any extra corrections. The Fourier space behavior of the 3rd-order B-spline scaling function enables it to be able to accurately recover the true power spectrum with errors less than 5% up to $k \leq k_N$. It is expected that such a method can be applied to higher order statistics in Fourier space and will enable us to have a precision capture of the non-Gaussian features in the large scale structure of the universe.

Key words: large scale structure of universe — methods: numerical

1 INTRODUCTION

The power spectrum is one of the most important statistical measures of the clustering strength of large scale structures. It encodes rich information about the physical universe as well as the structure formation. In the current CDM paradigm of hierarchical clustering driven by gravitational instability, the power spectrum reflects the typical scales of physical processes in the structure formation, while its positive-definiteness enables us to place tight constraints upon the majority of cosmological parameters and distinguish various theoretical models. Accordingly, the precision measurement of power spectra has been a central issue in the statistical study of the large scale structure of the universe.

Realizing the importance of the power spectrum in characterizing how galaxies cluster was initialized by Yu & Peebles (1969). Since then, the power spectra of galaxies has been measured for a number of redshift surveys, notably the CfA and the Perseus-Pisces redshift surveys (Baumgart & Fry 1991), the radio galaxy survey (Peacock & Nicholson 1991), the CfA redshift survey (Park et al. 1994), the QDOT survey (Feldman, Kaiser & Peacock 1994), the 1.2 Jy IRAS survey (Fisher et al. 1993), the 2 Jy IRAS survey, (Jing & Valdarnini 1993), the CfA and SSRS extensions (Vogeley et al. 1992; da Costa et

* Supported by the National Natural Science Foundation of China.

al. 1994), the Stromlo-APM redshift survey (Tadros & Efstathiou 1996) and the Las Campanas survey (Lin et al. 1996). Also, the real-space power spectrum has been extracted from the APM Galaxy Survey (Baugh & Efstathiou 1993, 1994) by inversion of both the angular correlation and 2-D power spectrum. In particular, the Fourier analysis of the 2dFGRS (e.g. Percival et al. 2002) and the SDSS (e.g. Tegmark et al. 2004; Percival et al. 2007) directly flags the epoch of precision cosmology.

The first practical method for measuring the power spectrum using a 3-dimensional redshift survey was described by Baumgart & Fry (1991). They pointed out that one can simply measure the galaxy power spectrum by enclosing the survey volume in a box and Fourier transform the data. In the most influential paper by Feldman, Kaiser & Peacock (1994), they proposed a variant to the one of Baumgart & Fry (1991), in which each galaxy is assigned a weight computed from an auxiliary random sample to account for the selection function and the window function so that the estimator reaches an optimal value.

For a given galaxy distribution, the Fourier transformation is evaluated directly by the trigonometric summation

$$\hat{\rho}_g(\boldsymbol{n}) = \sum_{i=1}^{N_g} w_i e^{2\pi \boldsymbol{n}\cdot\boldsymbol{x}_i/L} , \tag{1}$$

where $\boldsymbol{x}_i$ is the position of the ith galaxy, w_i is its weight, and N_g is the total number of galaxies in the catalog. The power spectrum is then $|\hat{\rho}_g(\boldsymbol{n})|^2$. The direct summation can only be calculated for a few thousand of galaxies; a more efficient approach is to use Fast Fourier Transformation (FFT) so that it is computationally feasible to analyze an extremely large number of objects. In order to apply the FFT technique, essentially one needs to partition the discrete particle distribution onto a grid, which is referred to mass assignment or binning. The binning procedure consists of a convolution of a distribution with a binning function W and the subsequent sampling on a finite number of grids. It is well known that the binning will result in spurious features in the Fourier power spectrum at scales around the Nyquist frequency of the FFT grid (e.g., Percival & Walden 1993; Baugh & Efstathiou 1994). Explicitly, we have,

$$|\hat{\tilde{\rho}}_g(\boldsymbol{n})|^2 = \sum_{n'=-\infty}^{\infty} |\hat{W}(\boldsymbol{n} + L\boldsymbol{n'})|^2 |\hat{\rho}_g(\boldsymbol{n} + L\boldsymbol{n'})|^2 . \tag{2}$$

The FT of the smoothed density, $\hat{\tilde{\rho}}_g(\boldsymbol{n})$ is generally not equal to $\hat{\rho}_g(\boldsymbol{n})$. The binning effect relies on the slope of the true power spectrum, thus the correction for this effect is model-dependent (Peacock & Dodds 1996). In a recent paper, Jing (2005) suggests an iterative method to reconstruct the true power spectrum from the alias sum Equation (2). Very recently, Cui et al. (2008) discussed in detail the sampling effects that the mass assignment scheme can bring to the measurement of the true power spectrum using FFT: smearing effect, aliasing effect and anisotropic effect. Rather than try to iteratively correct the aliasing effect, they proposed using particular mass assignment schemes that have minimum sampling effects.

During the last decade, algorithms for the fast evaluation of summation Equation (1) have also been developed and rendered in numerous applications in numerical analysis and statistics. Early efforts of implementation include Lagrange interpolation method (Press & Rybicki 1989; Brandt 1991), and Taylor expansion to correct for deviations from an equally spaced grid (Sullivan 1990). However, these approaches do not provide a very efficient algorithm, especially in multi-dimensional space. A much faster algorithm was suggested by Dutt & Rokhlin (1993) by generalizing the interpolation with Gaussian bells. Within the framework of multi-resolution analysis (MRA), Beylkin (1992) proposed an approach for the fast evaluation of the Fourier transformation of singular functions, which indeed furnishes a simple and efficient algorithm for Unequally Spaced Fast Fourier Transformation (USFFT). A similar approach, called space adaptive FFT, was presented by Fang & Feng (2000). In this paper, we will discuss the merits of using the mass assignment scheme based on the model of Beylkin (1992) in measuring the power spectrum with FFT.

The structure of this paper is organized as follows. In Section 2, we will briefly introduce the Beylkin's unequally spaced FFT algorithm for an irregular data set. Then, the mass assignment using B-spline scaling functions is presented with its advantages for estimating a power spectrum. In Section 4, we demonstrate its numerical performance calibrated by Poisson random samples and the Virgo N-body simulation sample. Summary and concluding remarks are in Section 5.

2 BEYLKIN'S ALGORITHM FOR UNEQUALLY SPACED FAST FOURIER TRANSFORM

Without loss of generality, all of the formulae hereafter are written in one-dimensional forms since the generalization to multi-dimensional space is straightforward. In general, we need to evaluate the trigonometric summation

$$\hat{n}(\xi) = \sum_{i=0}^{N_g-1} w_i e^{i2\pi\xi x_i} \tag{3}$$

for the data set $\{w_i\}_1^{N_g}$ in configuration of $x_i \subseteq [0,1]$. For a galaxy distribution, $\{x_i\}$ are positions of the galaxies and $\{w_i\}$ are their weights. Equation (3) can be written in an alternative form,

$$\hat{n}(\xi) = \int n(x) e^{i2\pi x\xi} dx\,, \tag{4}$$

with

$$n(x) = \sum_{i=1}^{N_g} w_i \delta_D(x - x_i)\,. \tag{5}$$

If we consider an extension of the period of $n(x)$, the 1-periodic function can be simply given by $\tilde{n}(x) = n(x - [x])$ in $\boldsymbol{R}$, here $[\cdot]$ denotes for integer part of a real number.

Now we can perform a multi-resolution analysis (MRA) (Daubechies 1992; Fang & Thews 1998) to express a certain function at various levels of spatial resolution, which forms a sequence of functional spaces $0 \subset \cdots \subset V_{-1} \subset V_0 \subset \cdots \subset L^2(\boldsymbol{R})$. Suppose a set of functions $\{\phi(x-k); k \in \boldsymbol{Z}\}$ form an orthonormal basis for V_0. These functions dilate by a scale 2^j and translate by $2^{-j}k$, so that they compose an orthogonal basis for V_j

$$\{\phi_{j,k}(x) = 2^{j/2}\phi(2^j x - k) \quad |k \in \boldsymbol{Z}\}\,, \tag{6}$$

and ϕ is called the basic scaling function. Projection of a function $f \in L^2(\boldsymbol{R})$ onto V_j is an approximation to f at scale j, and converges to f when $j \to \infty$.

In terms of scaling functions, we can decompose the density distribution $n(x)$ at scale j by

$$n(x) = \sum_k \epsilon_k^j \phi_{j,k}^P(x)\,, \tag{7}$$

in which $\phi_{j,k}^P(x)$ is the 1-periodic scaling function constructed such that

$$\phi_{j,k}^P(x) = \sum_{n=-\infty}^{\infty} \phi_{j,k}(x+n) = \sqrt{N} \sum_{n=-\infty}^{\infty} \phi(N(x+n) - k), \tag{8}$$

where $N = 2^j$. The scaling function coefficients (SFCs) $\{\epsilon_k^j\}$ are given by the inner product

$$\epsilon_k^j = \int n(x)\phi_{j,k}^P(x)dx \tag{9}$$

$$= \sqrt{N}\int_{-\infty}^{\infty} n(x)\phi(Nx - k)dx, \tag{10}$$

which describes the density fluctuation filtered on the scale of $k/2^j$ at position l (Fang & Thews 1998; Feng & Fang 2004) for $0 \le k, l \le N-1$. Taking the periodicity of the function $n(x)$, the domain of integration changes to $[0,1]$ and yields

$$\epsilon_k^j = \sqrt{N} \int_0^1 n(x) \sum_{l \in \boldsymbol{Z}} \phi(Nx - k - Nl) dx. \tag{11}$$

Using Poisson's summation formula, we have

$$\sum_{l \in \boldsymbol{Z}} \phi(Nx - k - Nl) = \frac{1}{N} \sum_{l \in \boldsymbol{Z}} e^{2\pi i (k - Nx) l/N} \bar{\hat{\phi}}(l/N), \tag{12}$$

and hence, in Fourier space, Equation (11) could be written in the form

$$\epsilon_k^j = \frac{1}{\sqrt{N}} \sum_{l \in \boldsymbol{Z}} \bar{\hat{\phi}}(l/N) \hat{n}(l) e^{2\pi i k l/N}, \tag{13}$$

with the Fourier transformation of $n(x)$ and $\phi(x)$ defined by

$$\hat{n}(l) = \int_0^1 n(x) e^{-2\pi i l x} dx, \tag{14}$$

and

$$\hat{\phi}(\xi) = \int_{-\infty}^{\infty} \phi(x) e^{-2\pi i x \xi} dx, \tag{15}$$

in which the symbol "$^-$" denotes the complex conjugate. Splitting the summation of Equation (13) into segments of length N gives

$$\epsilon_k = \frac{1}{\sqrt{N}} \sum_{l=0}^{N-1} \Big(\sum_{m \in \boldsymbol{Z}} \bar{\hat{\phi}}(l/N + m) \hat{n}(l + Nm) \Big) e^{2\pi i k l/N} . \tag{16}$$

Alternatively, we have

$$|F(l) - \hat{n}(l)| \le \sum_{m = \pm 1, \pm 2, \ldots} \frac{|\hat{\phi}(l/N + m)|}{|\hat{\phi}(l/N)|} |\hat{n}(l + Nm)|, \tag{17}$$

with

$$F(l) = \frac{1}{\sqrt{N} \bar{\hat{\phi}}(l/N)} \sum_{k=0}^{N-1} \epsilon_k e^{-2\pi i k l/N}. \tag{18}$$

Obviously, the summation in Equation (18) is taken over an integer grid and can be performed by standard FFT technique. If the scaling function is chosen in such a way that the left hand side of the above equation (Eq. (17)) is small enough, $F(l)$ provides a good approximation to $\hat{n}(l)$, and thus Equation (18) leads to a simple and efficient algorithm for evaluating the Fourier transformation of an unevenly sampled data set. In summary, it can be implemented in the following three steps,

(1) For a given density distribution $n(x)$, calculate the scaling function coefficients ϵ_k^j using Equation (10),

$$\epsilon_k^j = \sqrt{N} \sum_{i=1}^{N_p} w_i \phi^P (N x_i - k) . \tag{19}$$

Usually, the scaling function is chosen to have a compact support. In this case, the summation of cycling through the whole sample reduces adding up contributions from neighboring particles around position k.

(2) Perform the discrete Fourier transformation in Equation (18) by the standard FFT technique.
(3) Multiply the summation by the tabulated values of $1/\bar{\hat{\phi}}(l/N)$.

The efficiency of the algorithm rests on the scale dependence of the basis functions in both real and wave-number space; we will demonstrate that a higher order B-spline scaling function could be an appropriate choice, which will lead to a fast algorithm for given precisions.

3 MEASURING FOURIER POWER SPECTRUM VIA FFT

3.1 Mass Partition using B-spline Basis Functions

Mathematically, mass assignment tries to approximate the singular Dirac δ^D function with a set of basis functions. To achieve high computational efficiency, it is usually required that the window function have a compact support in real space, while for minimizing the aliasing effect, the window function shall be close to a top hat in Fourier space.

As noted by Beylkin (1992), the wavelets with compact support do not afford an efficient algorithm since the Fourier transformation of compactly supported wavelets does not decay fast enough. One good choice is to use a higher order B-spline which satisfies the requirement of localization in the real space and fast decay in wave-number space. In what follows, we will give a brief description of the basic properties of a n-th order B-spline, which will be useful in the implementation.

B-splines are symmetrical, bell shaped functions constructed from the $n+1$ fold convolution of a rectangular pulse $\beta^{(0)}(x)$:

$$\beta^{(0)}(x) = \begin{cases} 1 & \text{if } |x| < 0.5 \\ 0.5 & \text{if } |x| = 0.5 \\ 0 & \text{otherwise} \end{cases} \tag{20}$$

$$\beta^{(n)}(x) = (\beta^{(0)}_{+1} * \beta^{(0)}_{+2} * \cdots \beta^{(0)}_{+n} * \beta^{(0)}_{+(n+1)})(x), \tag{21}$$

where the symbol "$*$" denotes the operation of convolution. $\beta^{(n)}(x)$ is a piecewise polynomial of degree n. In practical calculations, the B-splines can be computed using recursion over the spline order,

$$\beta^{(n)}(x) = \frac{(n+1)/2 + x}{n} \beta^{(n-1)}(x + 1/2) + \frac{(n+1)/2 - x}{n} \beta^{(n-1)}(x - 1/2) \, . \tag{22}$$

Note that B-splines with $n = 0, 1, 2$ correspond to traditional mass assignment schemes: the Nearest Grid Point (NGP), the Cloud In Cell (CIC) and the Triangular Shaped Cloud (TSC), respectively.

The Fourier transformation of $\beta^{(n)}(x)$ is related to the $n+1$ fold convolution construction of the B-splines,

$$\hat{\beta}^{(n)}(\xi) = \Big(\frac{\sin \pi\xi}{\pi\xi}\Big)^{n+1} \, . \tag{23}$$

The n-th order B-spline has a compact support of $[-\frac{n+1}{2}, \frac{n+1}{2}]$. As β does not form an orthogonal basis, they could be part of a biorthogonal system. The corresponding dual scaling function can be constructed similar to that spanned by the B-splines. We apply the current orthogonalization scheme to construct its dual base γ,

$$\int_{-\infty}^{\infty} \beta^{(n)}(x-k)\gamma^{(n)}(x-l)dx = \delta_{kl} \, . \tag{24}$$

It follows from the above orthogonality condition that, in the wavenumber space,

$$\hat{\gamma}^{(n)}(\xi) = \frac{\hat{\beta}^{(n)}(\xi)}{a^{(n)}(\xi)} \tag{25}$$

with the periodic function

$$a^{(n)}(\xi) = \sum_{l=-\infty}^{\infty} |\hat{\beta}^{(n)}(\xi + l)|^2 = \sum_{l=-n}^{n} \beta^{(2n+1)}(l) e^{i2\pi l\xi} \, . \tag{26}$$

It is noticed that the dual scaling function γ is not compactly supported. Orthogonalizing the B-spline basis using the function $a^{(n)}(\xi)$ leads to the Battle-Lemarié scaling function in Fourier space,

$$\hat{\varphi}^{(n)}(\xi) = \frac{\hat{\beta}^{(n)}(\xi)}{\sqrt{a^{(n)}(\xi)}} \, . \tag{27}$$

It can be shown that, in terms of the Battle-Lemarié scaling function, the Dirac δ function could have a finite representation,

$$\delta^D(x-y) \to \sum_{k \in \boldsymbol{Z}} \varphi^n_{j,k}(x) \varphi^n_{j,k}(y) \, . \tag{28}$$

The above equation actually asserts the completeness of a set of basis functions, which is also a basic condition for mass assignment functions.

Taking the n-th B-spline as basis functions, it follows from Equation (16) that

$$\frac{F(\xi)}{\sqrt{a^{(n)}(\xi)}} = \hat{n}(\xi/N)\hat{\varphi}^{(n)}(\xi) + \sum_{l=\pm1,\pm2,\ldots} \hat{n}(N^{-1}(\xi+l))\hat{\varphi}^{(n)}(\xi+l) \tag{29}$$

with

$$F(\xi) = \frac{1}{\sqrt{N}} \sum_{k=0}^{N-1} \epsilon_k e^{-2\pi i \xi k} \, , \tag{30}$$

in which ϵ_k is the scaling coefficients decomposed in terms of B-spline functions.

In Figure 1, we compare the Fourier space behaviors, $W^2(\xi)$, of the traditional mass assignment schemes: NGP, CIC, TSC, and the Daubechies scaling function Daub6, as well as the 3rd-order orthogonalized B-spline functions, i.e., Bettle-Lemarié scaling function (BL 3rd), as indicated. The overlap region of $W^2(\xi)$ with $W^2(\xi-1)$ (or $W^2(\xi+1)$) indicates the strength of the aliasing effect. It is obvious that the FFT power spectrum based on mass assignment function with a perfect top-hat in Fourier space does not suffer from sampling effects. Thus, the best assembly of the Fourier window function $W^2(\xi)$ of 3rd-order Bettle-Lemarié scaling function to a top-hat ensures its best performance in measuring the true power spectrum with FFT.

3.2 Power Spectrum of Density Fluctuations

For a given cosmic density field $\rho(\boldsymbol{r})$, the density contrast $\delta(\boldsymbol{r})$ is defined by

$$\delta(\boldsymbol{r}) = \frac{\rho(\boldsymbol{r}) - \bar{\rho}}{\bar{\rho}} \, . \tag{31}$$

The cosmological principle ensures that $\rho(\boldsymbol{r})$ in a sufficiently large volume V_μ can be a fair representation of the overall cosmic field. The Fourier transform of $\delta(\boldsymbol{r})$ is simply

$$\delta(\boldsymbol{k}) = \frac{1}{V_\mu} \int_{V_\mu} \delta(\boldsymbol{r}) e^{i\boldsymbol{k}\cdot\boldsymbol{r}} d\boldsymbol{r} \, . \tag{32}$$

The power spectrum is defined by

$$P(\boldsymbol{k}) = \langle |\delta(\boldsymbol{k})|^2 \rangle \, , \tag{33}$$

where $\langle ... \rangle$ means the ensemble average.

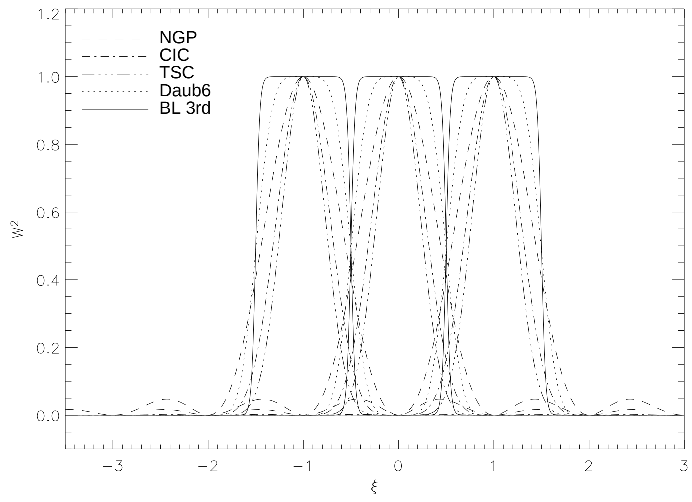

Fig. 1 Shapes of different mass assignment functions in Fourier space: the NGP (Nearest Grid Point), CIC (Cloud-In-Cell), TSC (Triangular Shaped Cloud), Daub6 (Daubechies 6) and BL 3rd (3rd-order Battle-Lemarié) mass assignment functions. Three sets of curves are of $W^2(\xi+1)$, $W^2(\xi)$ and $W^2(\xi-1)$, respectively.

A real galaxy catalog or data from an N-body simulation is a discrete realization of the underlying continuous density field; the number density could be written in the form of $n(\boldsymbol{r}) = \sum_i w_i \delta^D(\boldsymbol{r} - \boldsymbol{r_i})$, where $\boldsymbol{r}_i$ is the position of the ith object, w_i is its weight. For a flux-limited galaxy survey, w_i is specified by the selection function. The direct evaluation of the Fourier transformation of the discrete density field gives

$$\delta^d(\boldsymbol{k}) = \frac{1}{N}\sum_i w_i e^{i\boldsymbol{k}\cdot\boldsymbol{r_i}} - \delta^K_{\boldsymbol{k},0} \tag{34}$$

where N is the total number of objects and δ^K is the Kronecker symbol. It is easy to show that the true power spectrum can be measured simply by

$$P(k) \equiv \langle|\delta(\boldsymbol{k})|^2\rangle = \langle|\delta^d(\boldsymbol{k})|^2\rangle - \frac{1}{N} \tag{35}$$

Obviously, subtracting $1/N$ corrects for the shot noise in the power spectrum estimated from a sample of discrete objects. Practically, for a given mass assignment function, the measured power spectrum $P^{\rm fft}(\boldsymbol{k})$ computed by the FFT is related to the true one by

$$P^{fft}(\boldsymbol{k}) = \sum_{\boldsymbol{n}} |\hat{W}(\boldsymbol{k} + 2k_N\boldsymbol{n})|^2 P(\boldsymbol{k} + 2k_N\boldsymbol{n}) + \frac{1}{N}\sum_{\boldsymbol{n}} |\hat{W}(\boldsymbol{k} + 2k_N\boldsymbol{n})|^2 \tag{36}$$

where the summation is taken over 3D integer vector $\boldsymbol{n}$ and k_N is the Nyquist wavenumber. Comparing with Equation (35), the true power spectrum and shot noise are biased by $W^2(\boldsymbol{k})$ and its replicated aliasing terms.

In order to reconstruct the true power spectrum from the aliasing sum, Jing (2005) proposed an iterative method which has been shown to work well using N-body simulation tests. Here, we assert that the task can be accomplished in a more elegant way. If we adopt the 3-order B-spline scaling function for the mass assignment, as indicated in Figure 1, $|W(\boldsymbol{k})|^2$ resembles quite well a top-hat function in Fourier space within Nyquist sphere $|\boldsymbol{k}| \leq k_N$. This property ensures that the estimated power spectrum is hardly biased by the aliasing effect; therefore while using the FFT we can simply obtain the true power spectrum for a sample of discrete objects without any corrections besides the shot noise.

4 NUMERICAL TESTS

In this section, we will apply the Beylkin's algorithm to measure the power spectra of simulations to demonstrate its accuracy and performance.

4.1 Poisson Samples

For a Poisson random sample, the power spectrum $P_{\rm shot}(k) = 1/N$, where N is the number of particles. To test this, we generate 10 random poissonian samples, each of which consists of $N = 256^3$ particles randomly distributed in a cubic box. In Figure 2, we show the average values and 1σ errors of the power spectrum measured from these 10 samples. Note that since we do not input any additional power to the distribution of the random particles, the power spectrum measured using FFT contains only the second term in Equation (36). Different mass assignment schemes are employed to tabulate the grid density for comparison, including the three usually used mass assignment functions: NGP, CIC, TSC, as well as the unequally spaced Daubechies 6 (Daub6) and 3th-order B-spline scaling functions.

The upper and lower panels in Figure 2 correspond to the computations with 256^3 and 512^3 grids respectively. The results for each scheme are displayed using different symbols as indicated in the figure. According to Equation (36), the measured FFT power spectra for these Poisson random samples are $\frac{1}{N}\sum_{\boldsymbol{n}} |\hat{W}(\boldsymbol{k} + 2k_N\boldsymbol{n})|^2$, and should be $\langle NP_{\rm shot}(k)\rangle \equiv 1$ for the NGP, the Daub6 and the 3-order B-spline scaling functions, and much smaller than 1 for the CIC and TSC schemes. These are confirmed by the tests shown in Figure 2 based on calculations carried out on both the 512^3 and 256^3 grids.

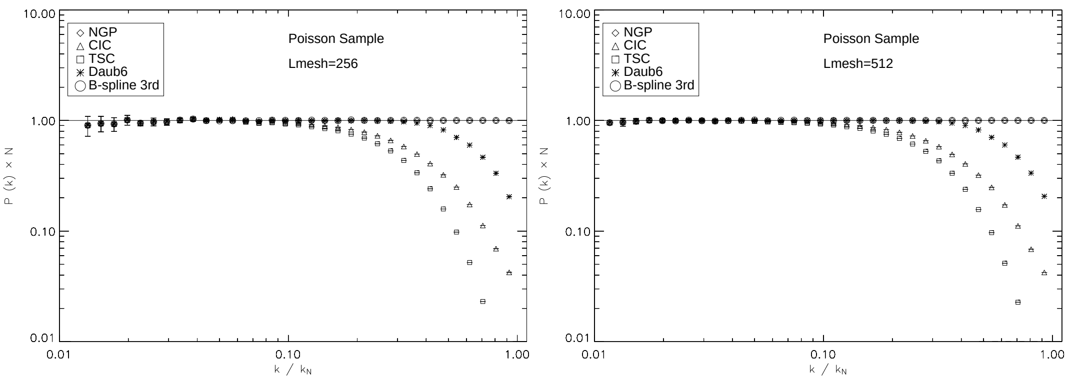

Fig. 2 The power spectra with 1-σ errors estimated from 10 Poisson random samples. Symbols as indicated in the figure represents the result using NGP, CIC, TSC, Daub6 and 3rd-order B-spline scaling functions for mass assignments upon a 256^3 grid (left panel) and a 512^3 grid (right panel).

4.2 Virgo Cosmological Simulation

We analyze the $z = 0$ output of an LCDM N-body simulation by the Virgo Consortium (Kauffman et al. 1999), where the cosmological parameters are $\Omega_m = 0.3$, $\Omega_\Lambda = 0.7$, $\Gamma = 0.21$, $h = 0.7$, $\sigma_8 = 0.9$ and its force soft length is $20h^{-1}$kpc. The simulation was evolved in a periodic cubic box of side length $239.5h^{-1}$Mpc with 256^3 CDM particles.

We measured the power spectrum of the Virgo sample in the same way as we did with Poisson samples, where the shot noise term (second term of Eq. (36)) is subtracted. Different scaling functions have been chosen, including the 3rd-order B-spline and the Daub6 scaling functions. For comparisons, we also make measurements using the NGP, CIC and TSC mass assignment schemes. The results for the

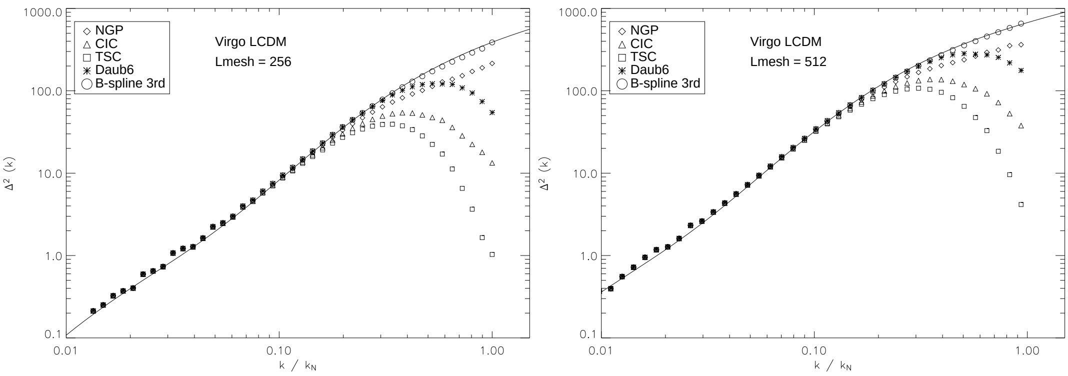

Fig. 3 The power spectra measured from the Virgo N-body simulation sample. Symbols as indicated in the figure are estimated with NGP, CIC, TSC, Daub6 and 3rd-order B-spline scaling functions for mass assignments upon a 256^3 grid (left panel) and a 512^3 grid (right panel).

dimensionless power spectrum $\Delta^2(k) \equiv 2\pi k^3 P(k)$ are presented in Figure 3, in which 256^3 (upper) and 512^3 grids (lower) have been used. To have a visual inspection of the accuracy achieved by different methods, we also plot the prediction using the fitting formula for a nonlinear power spectrum obtained by Smith et al. (2003) as solid lines.

Without correcting the smearing effect and the aliasing effect, the power spectrum obtained using the NGP, CIC and TSC algorithms significantly underestimated the true power spectrum. Both the results for Daub6 and 3rd-order B-spline scaling functions seem to work remarkably well at all scales up to $k \leq k_N$, and are in good agreement with the Smith et al. (2003) prediction.

To assess the precision of the Beylkin's algorithm, we examine the numerical errors of the power spectrum using the 3rd-order B-spline scaling function. In the case of computation with the 256^3 grid, the maximum errors are not more than 7% within the wavenumber range of k considered, meanwhile for those of the 512^3 grid, the error level is as low as $< 4\%$ even at $k \geq 0.6k_N$.

The power spectrum estimated from a discrete data set can be also recovered extremely well by the FFT technique based on B-spline scaling functions, capable of reaching the same level of accuracy without any corrections as the Jing's iteration correction algorithm. Another advantage is that it can be easily implemented with only minor modifications of those traditional methods. We conjecture that it can be further applied to estimate higher order cosmic statistics by Fourier analysis, for which there are no reliable methods available yet to compensate the aliasing. Moreover, we address the issue that although we have used the 3rd-order B-spline scaling function throughout this paper, in principle, the higher the order of the scaling function, the better the approximation to the Fourier transformation is. However, because the computational cost in a d-dimensional space scales as $(n+1)^d$ with the order of B-spline scaling function n, an algorithm with very high orders may be less efficient. To balance the two ends, we numerically tested the dependence of accuracy on the orders of B-spline scaling functions. Our result indicates that for $n = 3, 5, 7$, there are little differences at $k \leq k_N$. As the computational cost for a 3rd-order B-spline scaling function is $\propto 4^3$, slightly more than the TSC $\propto 3^3$, it suffices to use the 3rd-order B-spline scaling function for the power spectrum measurement.

5 CONCLUSIONS

Based on a well developed technique originally proposed by Beyklin, we described a new precise method for estimating the power spectrum of discrete samples. We demonstrate the efficiency and the accuracy of the algorithm with samples of N-body simulations. The prominent feature of this method is that the true power spectrum can be simply recovered without extra corrections for sampling effects of aliasing and anisotropics which resulted from mass assignment. The algorithm can be readily generalized to perform Fourier analysis of galaxy surveys to estimate not only the power spectrum of the density field, but also possibly of the peculiar velocity field.

Beyond the power spectrum in clustering analysis, the higher order statistics such as bispectrum and trispectrum quantify the non-Gaussian features produced by the highly non-linear mode-mode coupling. The precise measurements of non-Gaussian characters are helpful for discriminating among various models for the structure formation. Though a good numerical technique has been well developed for correcting the sampling effects in the precise measurements of the power spectrum (Jing 2005), practical algorithms enabling us to make accurate estimation of higher order spectra are still absent. It is expected that our unequally spaced FFT technique presented in this paper will provide an efficient tool to achieve such a goal. Moreover, by virtue of B-spline scaling functions, it can also be applied in performing N-body simulations.

Acknowledgements We thank the referee for providing constructive comments. This work is supported by the National Science Foundation of China through grants 10373012, 10633049, 10643002 and the 973 program under No. 2007CB815402. JP and XY would like to acknowledge the fellowships of the 100-talents program set up by the CAS. The simulation in this paper was carried out by the Virgo Supercomputering Consortium using computers based at the Computing Center of the Max-Planck Society in Garching and at the Edinburgh Parallel Computing Center. The data are publicly available at *http://www.mpa-garching.mpg.de/Virgo.*

References

Baumgart, D. J., & Fry, J. N. 1991, ApJ, 375, 25
Baugh, C. M., & Efstathiou, G. 1993, MNRAS, 265, 145
Baugh, C. M., & Efstathiou, G. 1994, MNRAS, 267, 323
Beylkin, G. 1992, SIAM J. Numer. Anal., 29, 1716
Brandt, A. 1991, Computer Physics Communications, 65, 24
Cui, W., Liu, L., Yang, X., Wang, Y., Feng, L., & Springel, V. 2008, ApJ, 687, 738
da Costa, L. N., Vogeley, M. S., Geller, M. J., et al. 1994, ApJ, 437, L1
Daubechies, I. 1992, Ten Lectures on Wavelets (Philadelphia, SIAM)
Dutt, A., & Rokhlin, V. 1993, SIAM J. Sci. Comput., 146, 1368
Fang, L. Z., & Feng, L. L. 2000, ApJ, 539, 5
Fang, L. Z., & Thews, R. 1998, Wavelet in Physics (Singapore: World Scientific)
Feng, L. L., & Fang, L. Z. 2004, ApJ, 601, 54
Feldman, H. A., Kaiser, N., & Peacock, J. A. 1994, ApJ, 426, 23
Fisher, K., Davis, M., Strauss, M. A., et al. 1993, ApJ, 402, 42
Jing, Y. P., & Valdarnini, R. 1993, ApJ, 406, 6
Jing, Y. P. 2005, ApJ, 620, 559
Kauffman, G., Colberg, J. M., Diaferio, A., et al. 1999, MNRAS, 303, 188
Lin, H., Kirshner, R. P., Shectman, S. A., et al. 1996, ApJ, 471, 617
Park, C., Vogeley, M. S., Geller, M. J., et al. 1994, ApJ, 431, 569
Peacock, J. A., & Nicholson, D. 1991, MNRAS, 253, 307
Peacock, J. A., & Dodds, S. J. 1996, MNRAS, 280, L19
Peebles, P. J. E. 1973, ApJ, 185, 413
Percival, D. B., & Walden, A. T. 1993, Spectral Analysis for Physical Applications (Cambridge: Cambridge University Press)
Percival, W. J., Sutherland, W., Peacock, J. A., et al. 2002, MNRAS, 337, 1068
Percival, W. J., Nichol, R. C., Eisenstein, D. J., et al., 2007, ApJ, 657, 645
Press, W. H., & Rybicki, G. B. 1989, ApJ, 338, 277
Smith, R. E., Peacock, J. A., Jenkins, A., et al. 2003, MNRAS, 341, 1311
Sullivan, T. D. 1990, Sandia Report
Tegmark, M., Blanton, M., Strauss, M., et al. 2004, ApJ, 606, 702
Tadros, H., & Efstathiou, G. 1996, MNRAS, 282, 1381
Yu, J. T., & Peebles, P. J. E. 1969, ApJ, 158, 103
Vogeley, M. S., Park, C., Geller M. J., et al. 1992, ApJ, 391, L5